

SYNTHESIS, CHARACTERIZATION AND PHOTOCATALYTIC APPLICATIONS OF *p*(AAc) MICROGELS AND ITS COMPOSITES OF Ni DOPED ZnO NANORODS

M. JAVED^a, S. HUSSAIN^{b,*}

^a*Department of chemistry, School of Science, University of Management and Technology, Lahore, Pakistan*

^b*Department of Chemistry, Lahore Garrison University, DHA Phase VI, Lahore, Pakistan*

ZnO nanorods and Ni doped ZnO nanorods with various concentration of nickel 0%, 5%, 10%, 15%, 20%, 25% were prepared by co-precipitation method. By added zinc acetate dehydrate and nickel nitrate as zinc and nickel precursor in presence of Ammonia solution. Microgels of *p*(AAc) and its composites of Ni doped ZnO nanorods were synthesized by inverse phase polymerization method under N₂ gas atmosphere. Optical structure and morphology of Ni doped ZnO nanorods and its composite with *p*(AAc) were determined by XRD, TEM, SEM, FTIR and UV-Visible spectrometer. The photocatalytic activity of the samples was testified by using Tungsten lamp of 500 W via photo-degradation of methylene blue (MB) as a standard dye. It was observed that the composite of *p*(AAc) microgels with Ni doped ZnO nanorods show much enhanced photocatalytic performance as compared to any other individual particle acting as alone. The enhanced photocatalytic activity is due to enhanced surface area, surface roughness and decreasing band gap.

(Received October 13, 2019; Accepted March 17, 2020)

Keywords: ZnO nanorods, Ni doping, *p*(AAc) microgels, Characterization, Photocatalytic

1. Introduction

Nanosized materials have been largely studied within the past few decades and are considered very important subject in the applied as well as basic sciences [1-3]. When the size of material reaches to the nano level then its surface area is increased and such a material finds commercial applications in drug delivery, antimicrobial bandages, disinfectants, in diagnostic techniques, biological imaging, solar cells, sun screens and photoelectronic devices [4-6]. The properties of nanostructures depend upon their structure, size, shape and topography; the photocatalytic activity mainly depends upon size and surface morphology [4]. Nanostructures may be organic (e.g. black carbon, bucky balls, and multiwall carbon nanotubes) or inorganic (e.g. metal oxides such as ZnO, NiO, TiO₂, AgO and CuO). By adding impurities in pure metal oxides their superconducting, ferromagnetic, magnetic, electrical and optical properties are improved. ZnO nanostructure has received special attention due to their significant performance in electronics, photonics, optics and biomedical applications [7]. ZnO is a wide band gap (3.37eV, binding energy of 60 meV) semiconductor material [8-10] and is considered to be the best among many other oxide semiconductors. The ZnO nanoparticles possess significantly higher antimicrobial potential as compared to the other metal oxide nanoparticles [8]. Due to their ease of syntheses, low cost and nontoxic nature, ZnO nanoparticles find various applications in solar cells, fuel cells, gas sensors and photo-catalysis [7]. They also demonstrate many interesting properties such as electron transport, gas sensing, field emission and luminescence [11]. They also find applications in the field of optical sensing devices due to their photo catalytic activity and thermal stability [12]. The photocatalytic activity of zinc oxide and metal doped zinc oxide nanoparticles is increased by increasing the surface area [13]. ZnO nanorods find applications in field of semiconductors used as gas sensors [14]; their fabrication is used to produce improved performance photoelectronic devices [15]. The ZnO nanostructures are of particular interest due to

* Corresponding author: dr.shabbirhussain@lgu.edu.pk

their wide band gap, biocompatibility, ease of synthesis and fabrication [16] and are under investigations in the form of nanocages, nanobelts, nanobridge, nanorings, nanocombs, nanowires, nanorods *etc* [17, 18]. Microhydrogels have become a very important and interesting material in hydrogels–bioapplications [19]. Hybrid microgels are obtained from combination of smart polymer, microgels and several nanoparticles and nanorods. On the basis of responsive behavior microgels are classified as temperature sensitive microgels, pH sensitive microgels, glucose responsive microgels, ionic strength sensitive and multi sensitive microgels [20]. Dyes are usually non-biodegradable and could not be removed from water directly. Absorption of photon of specific wavelengths causes the breakage and degradation of a molecule to break into smaller pieces [21]. The photocatalytic degradation of dyes in presence of sunlight is highly important for both fundamental and particle studies due to the mechanism for the removal of dye pollutants. Due to large surface area and uniform size of nanoparticles photocatalytic reactions takes place on catalyst surface. But the recovery of nanoparticles is very difficult from water. To overcome this problem nano-composite may be used to enhance the dye degradation activity and easy removal from water in the form of suspension [22]. Photocatalytic degradation of different dyes by Ni doped ZnO nanoparticles can be determined by UV spectrophotometer. Exposure of UV radiation causes photo oxidative degradation in which polymer chain is broken down into free radicals and their mechanical properties are changed.

Photocatalytic degradation of metal doped nanoparticles depends upon the formation of active oxidation species and the samples to be used. In the present study, the Ni doped ZnO and the composite with p(AAc) microgels were illuminated in light which resulted in the jumping of the electrons from VB (valance band) to CB (Conduction band) by generating holes and electrons that lead to the generation of highly oxidizable species which was used to degrade the dyes or color pigments. For the determination of structure, size and morphology of unknown compound several characterization technique such as XRD, FTIR, SEM, TEM and UV visible spectroscopy were used.

2. Experimental

2.1. Apparatus and chemicals

The chemicals used in the synthesis of microgels or nanorods were of analytical grade. Cyclohexane (solvent), sorbitan (surfactant) and acrylic acid (monomer) were of CDH, Unichem and SRC grades, respectively. N,N'-Methylene bisacrylamide (MBA) cross linker, tetramethylethylenediamine (TEMED) accelerator and acetone were procured from Sigma-Aldrich. Analytical grade chemicals including ethylene blue (BDH England), nickel nitrate (Unichem), zinc acetate (Uni-chem), ammonia (Sigma Aldrich) and ammonium persulfate (APS) initiator (BDH England) were used.

All the instruments and glassware used in the synthesis of nanorods and nanocomposite of Microgel were calibrated. The glassware were properly washed with distilled water and dried in oven. Oven of Memmert Germany, UV- spectrophotometer of model JASCO-V-770, hot plate (temperature range of 370°C) of VELP scientific, analytical balance of model D432510556, centrifuge of Changzhou Guohua Electric Appliance CO., Ltd. and Florescent bulb of Tungsram brand were used.

2.2. Synthesis of Ni doped ZnO nanorods

Pure ZnO nanorods can be synthesized by wet chemical process at low temperature 80°C. In this process nickel nitrate and zinc acetate dehydrate is used as a raw material to form Ni doped ZnO nanorods ($Zn_{1-x}Ni_xO$, $x = 0.0, 0.05, 0.10, 0.15, 0.2$ and 0.25) with 0% (undoped ZnO), 5%, 10%, 15%, 20% and 25% Ni doping, respectively. Three solutions were prepared Solution A, Solution B, Solution C respectively. Solution A was prepared by addition of zinc acetate into 100ml distilled water. Solution B was prepared by adding nickel nitrate in 100ml distilled water. Solution A and Solution B were mixed together in 250 ml beaker to form a Solution C. The contents in this beaker were put on a magnetic stirrer constantly for 30 min at 80°C. Then ammonia solution was added drop wise in till its pH reaches to 11. In case of pure ZnO

nanoparticles solution became clear and sea blue color was obtained in case of Ni doped nano rods. After 2 hours precipitates of nanorods of different concentration 0%, 5%, 10%, 15%, 20%, 25% were separated by filtration and dried at 80°C for 2 hours in oven and powdered samples were collected.

Table 1 displays the list of molarity percentage of nickel nitrate and zinc acetate used as a precursor to synthesize Ni doped ZnO nanorods.

Table 1. Molarity percentage of nickel nitrate and zinc acetate used as a precursor to synthesize Ni doped ZnO nanorods.

Percentage	0%	5%	10%	15%	20%	25%
Zinc Acetate	0.1M	0.095M	0.090M	0.086M	0.091M	0.080M
Nickel nitrate	0M	0.005M	0.01M	0.013M	0.018M	0.02M

2nd method:

Ni doped ZnO debris was synthesized at room temperature by way of an electrochemical route. The electrolytic bath consisted of acetonitrile and tetrahydrofuran (THF) mixed in the ratio of 4:1, wherein high purity Ni doped Zn metal sheet (1cm × 1cm) and laboratory grade platinum sheet (1cm × 1cm) served as anode and cathode respectively. The capping agent tetra-trimethyl ammonium-bromide (TTAB) additionally served because the electrolyte. Electrolysis changed into performed in nitrogen atmosphere for some hours in regular contemporary mode (GPS-30D, 0-30V, zero-5A). Current density became maintained to acquire different sized of debris. The molarity of TTAB in the chemical tub became varied from 0.1 mM to 0.9 mM. The white Ni doped ZnO debris stay suspended within the solvent and separated *via* using centrifugation. On drying, a free flowing powder of Ni doped ZnO particles are received [23].

2.2.1. Annealing

Dry samples were kept in oven at 150-200°C by using crucibles for two hours.

2.3. Synthesis of p(AAc) microgels

Poly acrylic acid, p(AAc) microgels were prepared by inverse suspension polymerization, taking 100ml cyclohexane in a three-necked round bottom flask and pouring 1ml of sorbitan (surfactant) in it. Then the opening of flask was sealed with stopper and silicon tape and thereaction mixture was put into the magnetic stirrer. The mixture was purged for 15 min under N₂ gas to remove oxygen. Then 0.023g MBA (cross linker) in 5ml Acrylic Acid (monomer) was added into the flask followed by its stirring for 15 min. The reaction was initiate by adding 0.133g APS (initiator) in 1 ml distilled water into the flask. The reaction mixture was continuously stirred under N₂gas environment for 20 min and then 0.5ml TEMED (accelerator) was added to accelerate the synthesis of microgels. After 2 hours the supply of nitrogen was cut off and the reaction mixture was stirred overnight. After 12 hours, the microgels were filtered, washed with acetone and dried in oven at 70°C to collect dispersed microgels particles.

2.4. Synthesis of microgelcomposites

Composites of microgels were prepared by adding 10%,20%, 30%, 40% and 50% doped nanorodsseparately in 100 ml cyclohexane present in three necked flasks before adding Sorbitan and the mixtures were stired for 15 min.Then0.023g MBA in 5ml-6ml AAc and 0.133g APS in 1 ml distilled water were added it into the flask and the gas was purged constantly. After 15 min, 0.5-0.6ml TEMED was added to accelerate the synthesis of nanocomposite of microgels. Mixture was stirredcontinuously under N₂ environment to obtain fine disperse nanoparticles. After 12

hours, microgels were filtered, washed with acetone and dried in oven at 70°C and collected in sample bottles.

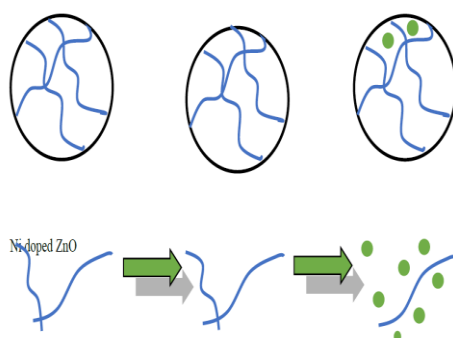


Fig. 1. Synthesis of micro gel Nanocomposite.

2.5. Photo catalytic degradation of nanorods

Photo catalytic degradation of methylene blue as standard dyewas carried out in presence of pure ZnO and doped ZnO nanorodswhich act as catalysts. For this purpose, 0.004g methylene blue was dissolved in 250ml flask to form a stock solution. After that 50ml of MB solution was taken in the beaker and placed under florescent bulb at the distance of 10cm vertically and 0.03 g of the catalyst (doped or undoped nanoparticles) was added in it while base line of UV-spectrophotometer was set by distilled water. After 30 min, 5ml of solution was pipette out from the beaker and centrifuged it for 1-2 min, poured the solution into cubit, placed it into the UV spectrophotometer and observed the absorbance.

2.6. Photo catalytic degradation of microgel and its composites

Composites of p(AAc)-ZnO-Ni act as a catalyst for the degradation of dye such as methylene blue. First of all, 50 ml of MB solution was taken from stock solution and 0.3 g sample was added into it. The UV – spectrophotometer was used to observe the reduction of methylene blue at different time intervals. Spectra for degradation were observed and confirmed by means of physical change from intense blue to colorless.

2.7. Sample Preparation

Weight percentage:

Percentage	0%	5%	10%	15%	20%	25%
Zinc Acetate	2.19g	2.08g	1.975g	1.887g	1.997g	1.75g
Nickel nitrate	0g	0.145g	0.29g	0.378	0.522g	0.581g

2.8. Synthesis of microgelcomposites

Total weight of microgel (Undoped) = 0.165g

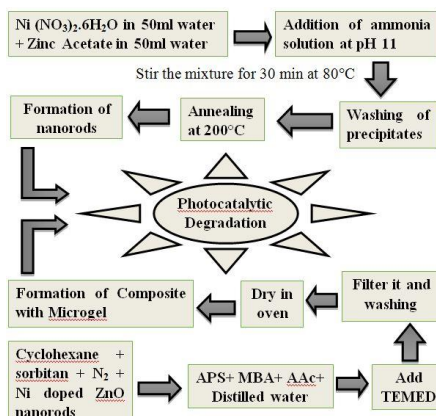
10% = 0.165g 10% nanorods in reaction mixture

20% = 0.033g 10% nanorods in reaction mixture

30% = 0.0495g 10% nanorods in reaction mixture

40% = 0.066g 10% nanorods in reaction mixture

50% = 0.0825g 10% nanorods in reaction mixture



Scheme 1 Flow sheet diagram for the synthesis of p(AAc) microgels And its composites.

3. Results and discussions

3.1. Scanning electron microscopy, SEM

The images of 5%, 15% and 25% sample of nickel doped ZnO nanorods shows sponges like grains with hexagonal structure. The morphology of ZnO and Ni doped ZnO were studied that clearly showed the size of nanorods increases when the concentration of dopant decreases from 25% Ni²⁺ to pure zinc oxide. The shape of nanostructures changes significantly from large surface to small rods as the concentration of doping is increased. SEM image clearly indicated the formation of small particles, few large particles and the small grain is agglomerated due to doping of nickel. Some kind of agglomeration is observed because of the presence of the force of attraction between the nanostructures due to increases in surface area to volume ratio. Fig 4.2 shows the SEM image of pure ZnO nanorods with some agglomeration. Fig 4.3 represents SEM image of 5% doped ZnO nanorods with decreasing their size by increasing surface area with some sort of agglomeration. SEM image of 15% doped ZnO nanorods is shown in Fig 4.4 with diameter less than 100nm, Fig 4.5 represents the image of 20% Ni doped zinc oxide nanorods.

3.1.1. SEM image of pure microgels

The morphology of p(AAc) microgels were studied by scanning electron microscope. SEM image of pure microgels of p(AAc) indicate a spherical microgels with some agglomeration with diameter less than 200nm. Fig 4.1.4 shows the formation of rounded microgels having some kind of agglomeration. Fig 4.1.5 represents the structure of 10% composites with p(AAc) microgels with some aggregation in it. Fig 4.1.6 shows the formation of 20% microgel composites with diameter 2-5µm. Fig 4.1.7, 4.1.8 also indicate the formation of p(AAc) microgel nanocomposite with some sort of agglomeration with diameter about 5-10µm.

3.2. Transmission electron microscopy

The TEM image of pure microgels indicates the formation of round shape porous nanostructures with size less than 200nm. These particles were finely dispersed with some agglomeration.

3.3. X-Ray Diffraction Techniques:

Nickel doped with zinc oxide nanoparticles show high susceptibility to agglomeration so it is really difficult to find out the actual size of nanoparticles by scanning electron microscope. The X-ray diffraction technique gives excellent explanation of the size of nanoparticles and nanorods. As the nickel doping concentration increases in ZnO from 5% to 25% then the size of nanostructure decreased. The major causes of size depletion of Ni doped ZnO is subsequent growth and suppression of nucleation. Nucleation was stopped due to the creation of interstitials by foreign impurities present in the sample. It is well known that the concentration of doping may cause

decreasing the size of nano structures but up to certain limit the size of nanoparticles increases after 20% nickel doping due to the effect of distortion around the dopant because of unequal ionic radii of Ni^{2+} and Zn^{2+} .

The samples of nickel doped zinc oxide nanoparticles and undoped ZnO having different concentrations exhibit no extra peak and the position of peaks was also same. The peaks which observed consisted of the signals of pure ZnO structure, and Ni doped nanorods. The range of diffraction angle was between 20° to 80° for XRD pattern to measure the size of undoped and doped nanorods.

3.3.1. XRD of ZnO nanorods

X-ray diffraction is a handy approach for figuring out the imply size of nano crystallites in nano crystalline bulk substances. This can be attributed to the fact that “crystallite size” isn't synonymous with “particle length”, while X-Ray diffraction is sensitive to the crystallite size inside the debris [24].

XRD spectrum of pure ZnO nanorods annealing at 200°C has been shown in the Figure 3. Highly intense diffraction peaks were observed around 100, 002, 101, 102, 110, 103, 112 planes. The diffracted values were 31.5° , 34.4° , 36.33° , 47.44° , 56.54° , 62.89° and 67.95° with their intensities 307.39, 278.19, 499.39, 127.59, 228.94, 187.52 and 193.63, respectively. Here the highest peak namely (101) has 2θ (diffracted) value (36.33°) for intensity 499.39. All seven peaks are characteristic of zinc oxide nanorods; the hexagonal wurtzite structure of crystal shows high crystallinity of Zinc oxide nanorods.

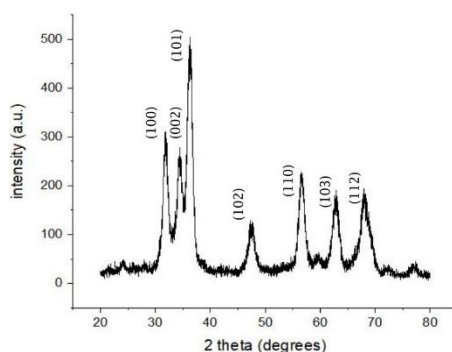


Fig. 3. XRD spectrum ZnO nanorods.

3.3.2. Competitive study of XRD pattern of ZnO and Ni-doped ZnO Nanorods with Different Wt. Percentages:

Diffraction peak increased with increasing the doping concentration and then start decreased due to degeneration the crystalline structure of ZnO with doping and increasing surface roughness which played an important role in photocatalytic degradation.

XRD pattern of Ni doped ZnO nanorods ($\text{Zn}_{1-x}\text{Ni}_x\text{O}$, where $x = 0.00$ to 0.25) annealed at 200°C several peaks was observed at 2θ diffracted at 31.7° , 34.5° , 36.2° , 47.4° , 56.5° , 62.7° , 67.8° and reflected at 100, 002, 101, 102, 110, 103, 112. At 101 a highly intense peak is observed due to crystalline structure of doped nanostructures.

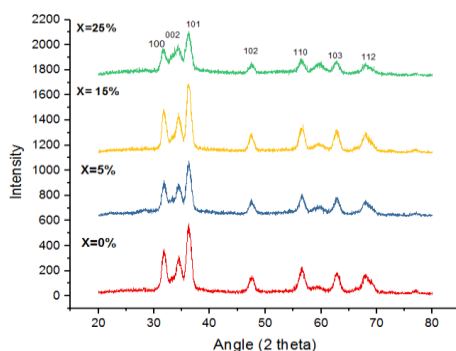


Fig. 4. XRD spectra for Ni doped ZnO nanorods.

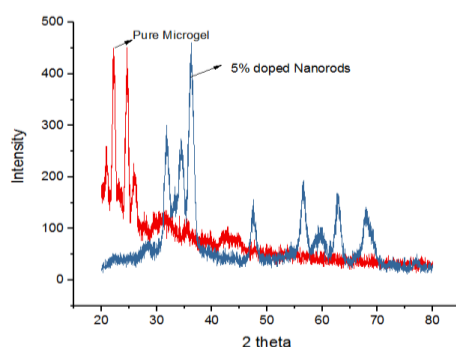


Fig. 5. XRD spectra for Microgel and 5 % Ni doped ZnO nanorods.

3.4. Fourier Transform infra-red spectroscopy

FT-IR spectra of Ni doped ZnO and its composite with microgel was used for conformation of its structure and different functional groups present in Ni doped ZnO nanorods and its composites with p(AAc) so the shape of Ni doped ZnO nanorods was changed when concentration of doping was changed which affects the intensity of the peaks.

3.4.1. FTIR spectra of Pure ZnO nanorods:

FTIR Spectra of pure ZnO nanorods shows a highly intense peak around 3487.02 cm^{-1} due to stretching vibrations of -OH group. A sharp band around 1574.61 cm^{-1} showed highly intense band due to bending vibrations of H-OH group which might be due to presence of water molecules in the surface of nanorods. A slightly broad band was observed near 3026.1 cm^{-1} due to the presence of organic structures. One more intense and sharp peak around 1475 cm^{-1} was observed due to presence of CH_3COO^- a sharp peak around 667.63 cm^{-1} was observed due to presence of zinc.

3.4.2. FTIR spectra of 5% Ni doped ZnO nanorods:

FTIR Spectra of 5% Ni doped ZnO nanorods is shown in figure below in which a peak around 3464.29 cm^{-1} was observed which indicate the stretching vibrations of -OH group. A band around 1475.77 cm^{-1} due to the presence of water molecules in the surface of nanostructures. A slightly broad band was observed near 3033.9 cm^{-1} due to the presence of organic structures. One sharper peak around 1393 cm^{-1} was observed due to presence of CH_3COO^- a sharp peak around 659 cm^{-1} was observed due to Ni^{+2} doping.

3.4.3. FTIR spectra of 15% Ni doped ZnO nanorods:

FTIR band of 15% Ni doped ZnO nanorods exhibited a peak around 1459.3 cm^{-1} which shows bending vibrations of H-OH group. A band around 1475.77 cm^{-1} indicated a sharp band because of bending vibrations of OH-H group. A peak around 3033.91 cm^{-1} was the indication of

organic structures present in dopant species. One sharp peak around 1393 cm^{-1} was observed due to presence of acetate group and a sharp peak around 626.9 cm^{-1} was observed due to Ni^{+2} doping.

3.4.4. FTIR spectra of 25% Ni doped ZnO nanorods:

FTIR spectra of 25% Ni doped ZnO was shown between the range $1000\text{-}4000\text{ cm}^{-1}$ for different Functional group in which highly intense peak around 659 cm^{-1} was observed that exhibited the doping of Ni^{+2} in the sample. The band was highly broad at the range of 3441 cm^{-1} due to -OH stretching and peak around 1484.4 cm^{-1} bending vibration of H_2O molecules. The peak around 2366.2 cm^{-1} was due to presence of (O=C=O) stretching. Stretching vibration were observed around 3033.9 cm^{-1} due to C-H bonding. The peak around 1245.1 cm^{-1} was observed due to presence of NO_3^- in nanorods.

3.4.5. FTIR spectra of pure microgel:

FTIR spectra of p(AAc) microgel were identified between $4000\text{-}400\text{ cm}^{-1}$ for the identification of several functional groups present in samples at various positions. For pure microgel Nano-composites the peak around 3026.1 cm^{-1} due to C-H (Anti-symmetric stretching) and highly intense peak around 1706.2 cm^{-1} was due to acid stretching (C=O) is observed. A small peak also observed around 1245.1 cm^{-1} because of C-O stretching vibrations. Amide stretching was observed between 1591 cm^{-1} to 1706 cm^{-1} in FTIR region.

3.4.6. FTIR spectra of 10% microgel composites:

FTIR spectra of 10% Ni-ZnO-p(AAc) microgels nano-composite was observed by FTIR spectroscopy between the range of $4000\text{-}400\text{ cm}^{-1}$ for the recognition of different functional groups present in composites at different positions. For 10% Nano-composites the peak around 3038.1 cm^{-1} are observed due to C-H (Anti-symmetric stretching) and highly intense peak around 1738.71 cm^{-1} was due to carbonyl (C=O). A band around 1256 cm^{-1} is observed because of C-O (stretching vibrations) and Amide stretching is observed at 1499 cm^{-1} in FTIR region. The peak around 683.93 cm^{-1} was observed due to the Ni^{+2} group and sharp peak around 551.84 was observed due to ZnO nanostructure.

3.4.7. FTIR spectra of 20% composites:

The spectra of 20% Ni doped ZnO with p(AAc) microgel nanocomposite was observed between the range of $4000\text{-}400\text{ cm}^{-1}$ for pointing out different F.G present in nano-composites at different locations. The intense peak around 677.4 cm^{-1} and 551.8 cm^{-1} were observed for 20% Nano-composites due to the Ni^{+2} doping with ZnO. The intense peak around 3038.03 cm^{-1} was spot to C-H (Anti-symmetric stretching) and intense band around 1738.71 cm^{-1} because of carbonyl (C=O) groups in polymers of AAc microgels. A very sharp peak around 1250 cm^{-1} was pointed due to stretching vibration of C-O group. Stretching of amide was observed at $1417\text{-}1494\text{ cm}^{-1}$.

3.4.8. FTIR spectra of 30% composites:

FTIR spectra between the ranges of $500\text{-}4000\text{ cm}^{-1}$ for 30% composites in which several peaks was observed for the determination of functional group and chemical structures of composites. A peak around 677.4 cm^{-1} was observed due to Ni^{+2} doping. The peak around 3042.5 cm^{-1} was analysed due to (Anti-symmetric stretching) of C-H group. The highly intense band around 1732.67 cm^{-1} was observed due to carbonyl group. A sharp band around 1255.1 cm^{-1} was observed due to C-H stretching vibrations.

3.4.9. FTIR spectra of 40% Composites:

In the case of 40% composites band ranges between $400\text{-}500\text{ cm}^{-1}$ was observed for identification of functional group. A peak pointed on 677.4 cm^{-1} is due to Ni^{+2} doping. The peak around 3143.9 cm^{-1} is observed due to (Anti-symmetric stretching) of C-H group present in fabricated microgels nano-composite. The highly intense band around 1732.49 cm^{-1} is observed due to C=O group. An intense peak around 1254.96 cm^{-1} is observed due to (stretching vibrations) of -CH group. The peak around 550 cm^{-1} is also observed due to ZnO stretching present in given sample.

Table 5. Comparison of Observed FTIR spectra of doped ZnO nanorods and p(AAc) microgel.

Functional group	Litrature Value	Observed peak for Ni doped ZnO	Observed value for P(AAc)	Observed value for p(AAc) Composites
O-H streaching	3421 cm ⁻¹	3464.29 cm ⁻¹	3462.98 cm ⁻¹	
Organic structures	2927-2980 cm ⁻¹	3032.04 cm ⁻¹	3031.81 cm ⁻¹	3038 cm ⁻¹
C=O Streaching	1637 cm ⁻¹	1706.24 cm ⁻¹	1703.13 cm ⁻¹	1738.7 cm ⁻¹
O-H bending vibrations	1459.1-1587.47 cm ⁻¹	1586.13 cm ⁻¹	1459.3 cm ⁻¹	1494 cm ⁻¹
CH ₃ COO- component	1357 cm ⁻¹	1338.93 cm ⁻¹	1274.66 cm ⁻¹	1250.3 cm ⁻¹
Ni ⁺² doping	667 cm ⁻¹	660.86 cm ⁻¹	659.8 cm ⁻¹	667.4 cm ⁻¹
Antisymmetric vibration of COO ⁻	1260 cm ⁻¹	1261.10 cm ⁻¹	1245.1 cm ⁻¹	1250 cm ⁻¹
ZnO streaching	550 cm ⁻¹	551cm ⁻¹	-	551.8 cm ⁻¹
Isopropyle streaching	1367 cm ⁻¹		1459.3 cm ⁻¹	1417 cm ⁻¹
NH Streaching	1534 cm ⁻¹	1459.3 cm ⁻¹	1591 cm ⁻¹	1533.91 cm ⁻¹

3.5. Photocatalytic Degradation:

UV spectra of Pure and Ni doped ZnO nanorods indicated a remarkable variation in blue region of UV spectra. The conduction band was combined with Fermi level because of high level of carrier concentration. Band gap of Ni doped ZnO has 3.16eV and ZnO has 3.31eV respectively. The decreased in absorption intensity and band gap was due to doping of Ni which increases effective sites and surface area in nanorods. Photocatalytic degradation of nanorods was switched out by using UV light and methylene blue was used due to its absorption if UV region [25].

In the presence of light and absence of catalyst methylene blue was not able to reduce completely so pure zinc oxide and Ni doped zinc oxide nanorods were used as a catalyst for degradation of dye (MB) but these metallic nanostructures ZnO-Ni was not working efficiently or effectively so p(AAc)-ZnO-Ni microgelsnano-composite was helpful and very efficient for photocatalytic degradation and very less amount of time is required to degrade it completely.

3.5.1. Degradation of MB by pure ZnO nanorods:

Metallic nano- structures of Zinc oxide (ZnO) was very effective specie used for degradation of MB at different intervals of time by taking 0.03gcatalyst in it. Graph shows that increasing concentration of ZnO nanorods in the reaction mixture leads to degraded it faster but upto certain limit then it shows maximum absorption.

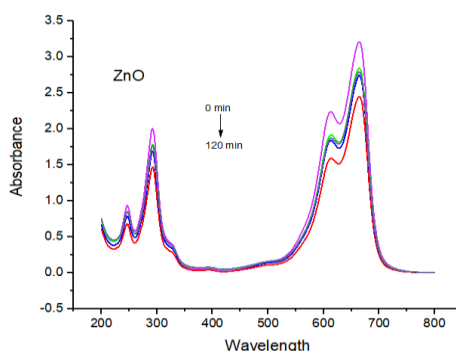


Fig. 4.5 Degradation of MB by pure ZnO nanorods.

3.5.3. Degradation of MB by 5% or 10% Ni doped ZnO nanorods:

Degradation of methylene blue by using 0.3g of 5% or 10% nickel doped nanostructures in a reaction mixture shown in figure below in which maximum absorption was observed. After the time intervals of 30 minutes take 5-6 ml of sample and centrifuged and UV-Vis spectra were determined to enhance photocatalytic activity since concentration of MB was decreased due to irradiation of UV-light as shown in the following Fig. below:

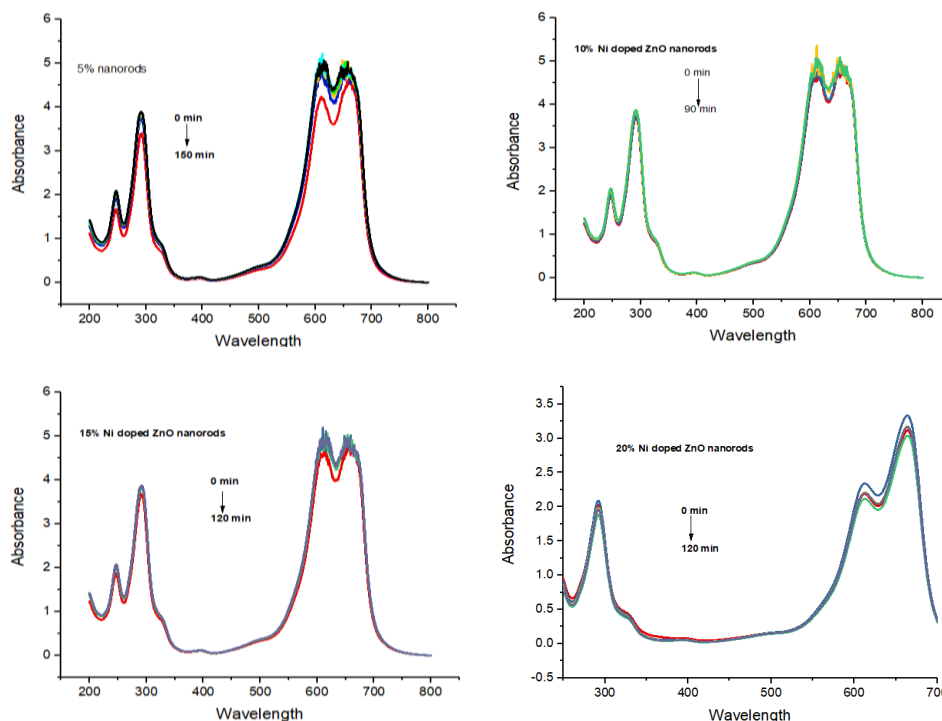


Fig 4.5.1. Degradation of MB by 5%, 10%, 15% and 20% Ni doped ZnO nanorods.

3.5.4. Degradation of MB by 15% or 20% Ni doped ZnO nanorods

Degradation of MB by taking 0.3g of 15% or 20% Nickel doped nanorods in a reaction mixture. After the regular time intervals of 30 minutes took 5-6 ml of sample and centrifuged and UV-Vis spectra were determined to enhance photocatalytic degradation since concentration of MB was decreased due to irradiation of UV-light as shown in the following Figure below.

3.5.5. Degradation of MB by Ni doped ZnO nanorods after 30 min:

Ni doped ZnO nanorods used to degrade the dyes present in industrial waste and waste water. The photocatalytic activity of doped nanostructure with different molar ratio of nickel after the regular interval of 30 min take 5-6 ml of sample and centrifuged as shown in figure that indicate 5% or 10% Ni doped ZnO nanostructures degrade faster than 15%, 20%, 25% or pure ZnO nanorods.

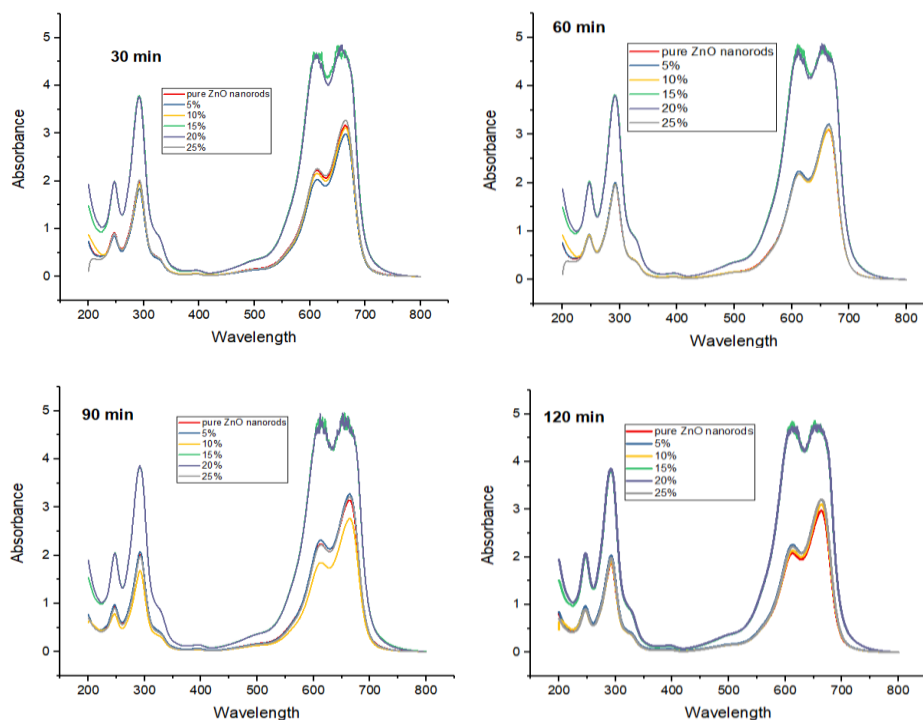


Fig. 4.5.2. Degradation of MB by different percentage of nanorods after 30, 60, 90 and 120 min.

3.5.6. Degradation of MB by Ni doped ZnO nanorods after 60 min:

Photocatalytic activity of different concentration of synthesized Ni doped ZnO nanorods was determined by the degradation of methylene Blue. For this, 0.03 grams of 5%, 10%, 15%, 20%, 25% Ni-doped ZnO nanorods were used. After 1 hour the photocatalytic degradation of MB solution of different percentage was observed in presence of UV-light in which 5% or 10% Ni doped ZnO degrade at the same rate but Ni doped ZnO nanorods with higher concentration of dopant did not degraded because of band gap of Ni doped ZnO decreases by increasing its active sites and surface defects that leads to absorption in visible region.

3.5.7. Degradation of MB by Ni doped ZnO nanorods after 90 min

Photocatalytic activity of different concentration of synthesized Ni doped ZnO nanorods was determined by the degradation of methylene blue solution. For this purpose 0.03 grams of 5%, 10%, 15%, 20%, 25% Ni-doped ZnO nanorods were taken in MB solution present in five different beakers of 100ml. After 90 min methylene blue was degraded by 10% Ni doped ZnO nanorods very efficiently than 5%, 15%, 20%, 25% nanorods because of increasing its surface area and surface defects.

3.5.8. Degradation of MB by Ni doped ZnO nanorods after 120 min

Methylene blue is degraded by 10% doped nanostructures very effectively than 15%, 20%, 25% Ni doped ZnO nanostructures due to increasing its surface area and active sites due to this absorption will shift towards visible region.. After 120 min at room temperature methylene blue degrade itself in presence of UV light by metallic catalyst.

3.5.9. Degradation of methylene blue by p(AAc) microgel

Pure p(AAc) microgel degraded itself in the presence of UV light falling vertically on the sample. Pure microgel is not degraded efficiently in UV-Visible region.

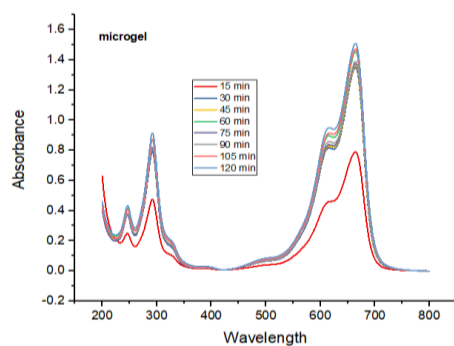


Fig. 4.5.6 Degradation of Methylene blue by p(AAc) Microgel.

3.5.10. Degradation of MB by p(AAc) microgel composites:

Degradation of dyes or color pigments takes place in the presence of UV-light and the instrument used to study the process of degradation is UV-Spectrophotometer and the branch of science that deals with the study of spectra is known as spectroscopy. Different samples of composites of microgels Ni-ZnO p(AAc) are taken to determine their effects of degradation on dye. The concentration of doped nanostructures is 10%, 20%, 30%, 40% in pure p(AAc) microgel prepared at room temperature under optimum conditions in N_2 gas environment.

Degradation process has been studied till 90 min or after the interval of every 15 min. MB was degraded by composites of microgel in the first 30 min after that it cannot be degraded efficiently after that.

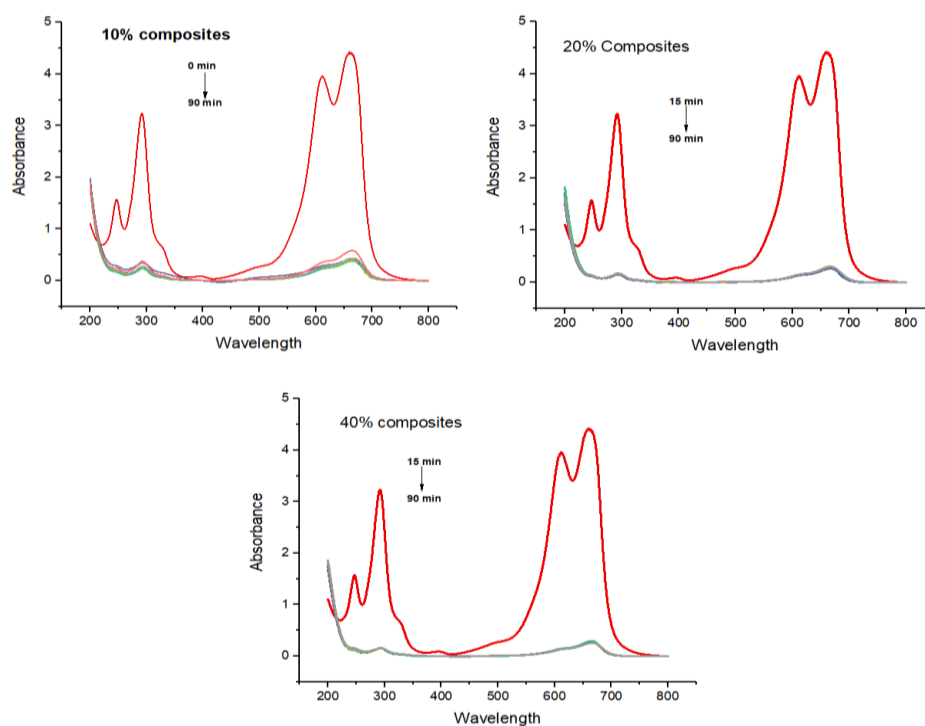


Fig. 4.5.7. Degradation of MB by 10, 20 and 40% composites.

3.5.11. Degradation of MB by different concentration of p(AAc) microgel composites:

Poly Acrylic acid microgel was an active catalyst used to degrade the methylene blue solution. Composites of p(AAc) microgels can be prepared by different concentrations of Ni-doped nanostructures in the reaction mixture, i.e., 0%, 10%, 20%, 30%, 40% respectively. 20% composites of microgel give us the best results among any other samples in almost 30-60 minutes.

Degradation of MB is studied till 120 min for the complete analysis of degradation of MB under UV light.

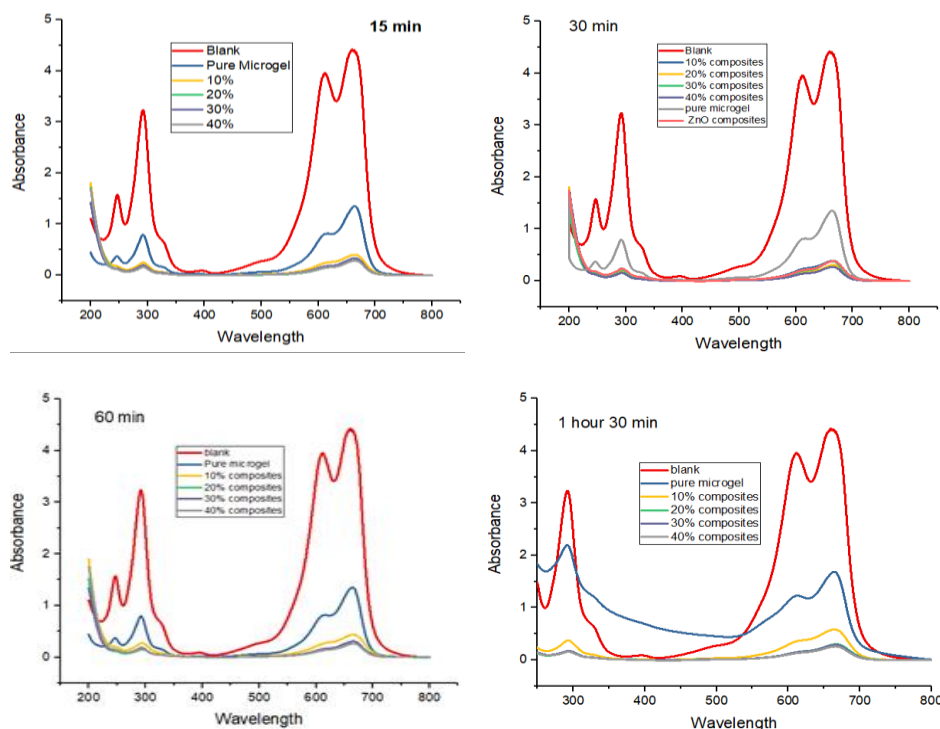


Fig. 4.5.10. Degradation of MB by different concentration of composites after 15, 30, 60 and 90 min.

3.5.11. Comparative study of photocatalytic degradation:

Transition metals doped with sub group III – V by changing the band gap between dopants photocatalytic activity of Ni-ZnO-p(AAc) nanostructures is checked by methylene blue as a standard dye which is the major pollution causing agent in waste water at room temperature. By using $Zn_{1-x}Ni_xO$ (0.00, 0.05, 0.10, 0.15, 0.20, 0.25) we observe methylene blue degraded slightly due to increasing its surface area, reducing band gaps and increasing their active sites but composites of microgels with (10%, 20%, 30%, 40%) doped nanorods degraded efficiently in presence of UV radiations. Among these composites of microgel, 20% composites gives very good photocatalytic degradations.

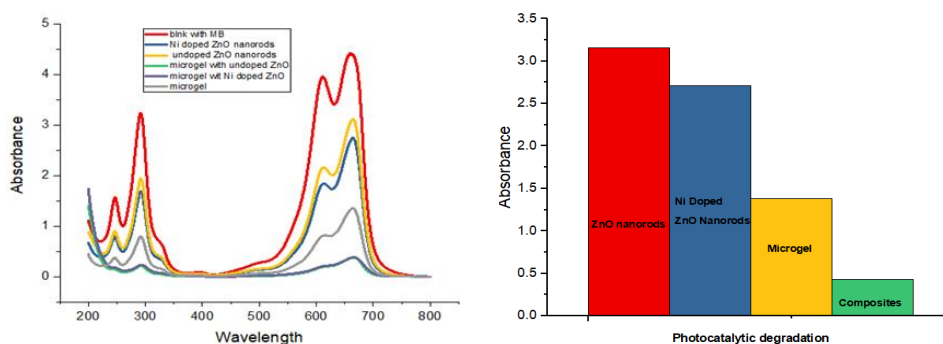


Fig. 4.5.13. Comparative study of absorbance of different nanostructure.

4. Conclusions

At 80°C Ni doped ZnO can be prepared by wet chemical process. P(AAc) microgels and its composites with Ni doped ZnO can be prepared by inverse phase polymerization under N₂ gas environment. TEM & SEM disclose the stability of p(AAc) and Ni doped ZnO nanorods due to very little agglomeration between them. FTIR and XRD spectra of microgels indicate the formation and stability of nanorods and nanocomposite with p(AAc) microgels. The composites of microgel having very good properties of photo-catalytic degradation of industrial dye of methylene blue.

The catalyst can be separated after the degradation mechanism. Hydrogels has very efficient adsorbent. The 20% composite of p (AAc) microgels used as adsorbent for MB shows good catalytic properties then pure microgels and Ni doped ZnO nanorods. Degradation of dyes is improved by Ni dopants with ZnO but efficiency of Ni-ZnO-p(AAc) composites is much higher than pure microgel or doped ZnO nanostructures. The ideal condition of dye degradation is at low pH with 0.8mg/50ml MB with 20% Ni-ZnO-p(AAc) nanocomposite in presence of UV-light. It has observed that 95% MB degraded within 1 hour by using 20% composite but 10% Ni doped ZnO degraded efficiently among 5%, 15%, 20%, and 25% dopant within 2 hours. Photocatalytic degradation of MB is attained with degradation in COD within 120 min.

References

- [1] C. Bhakat, P. P. Singh, International Journal of Modern Engineering Research **2**(4), 2452 (2012).
- [2] S. Mustansar et al., Electrochimica Acta **212**, 260 (2016).
- [3] M. Javed et al., Materials Science for Energy Technologies **1**(1), 70 (2018).
- [4] M. Valcárcel, B. Simonet, Nanomaterials for improved analytical processes. 2011, Springer.
- [5] L. Saad, M. Riad, Journal of the Serbian Chemical Society **73**(10), 2008.
- [6] O. Lupan et al., Physica status solidi A **205**(11), 2673 (2008).
- [7] S. Sabbiyola et al., Journal of Alloys and Compounds **694**, 522 (2017).
- [8] N. Jones et al., FEMS microbiology letters **279**(1), 71 (2008).
- [9] S. Xu, Z. L. Wang, Nano Research **4**(11), 1013 (2011).
- [10] S. Baskoutas, Materials **11**, 873 (2018).
- [11] G.-C. Yi, C. Wang, W. I. Park, Semiconductor Science and Technology **20**(4), S22 (2005).
- [12] J. Mikulski, et al., RSC Advances **6**(50), 44820 (2016).
- [13] M. S. Abdel-Wahab et al., Superlattices and Microstructures **94**, 108 (2016).
- [14] K. Harun et al., Procedia Chemistry **19**, 125 (2016).
- [15] Z. Ibusoto et al., Materials **6**(8), 3584 (2013).
- [16] G. Dar et al., Talanta **89**, 155 (2012).
- [17] W. L. Hughes, Z. L. Wang, Applied Physics Letters **86**(4), 043106 (2005).
- [18] X.-L. Yu, et al., Nanoscale research letters **5**(3), 644 (2010).
- [19] H. Kawaguchi, Stimuli-Sensitive Microhydrogels, in Biomedical Applications of Hydrogels Handbook. 2010, Springer. p. 107.
- [20] R. Begum, K. Naseem, Z. H. Farooqi, Journal of Sol-Gel Science and Technology **77**(2), 497 (2016).
- [21] E. Yousif et al., Journal of Taibah University for Science **11**(6), 997 (2017).
- [22] J. Li et al., Journal of molecular catalysis A: Chemical **261**(1), 131 (2007).
- [23] M. Bhuiyan, M. Rahman, Int. J. Res **3**, 67 (2014).
- [24] A. Monshi, M. R. Foroughi, M. R. Monshi, World journal of nano science and engineering **2**(3), 154 (2012).
- [25] S. Kant, A. Kumar, Adv. Mat. Let. **3**(4), 350 (2012).